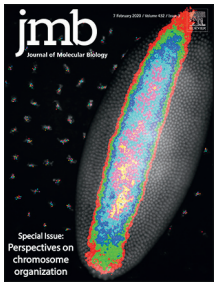

Mitochondrial Oxidative Stress Induces Rapid Intermembrane Space/Matrix Translocation of Apurinic/Apyrimidinic Endonuclease 1 Protein through TIM23 Complex

Arianna Barchiesi [1†], Veronica Bazzani [1†], Vanessa Tolotto [1], Praveenraj Elancheliyan [2,3], Michał Wasilewski [2,3], Agnieszka Chacinska [2,3] and Carlo Vascotto [1,2*]

*1 - **Department of Medicine,** University of Udine, 33100 Udine, Italy*
*2 - **Laboratory of Mitochondrial Biogenesis,** Centre of New Technologies, University of Warsaw, 02-097 Warsaw, Poland*
*3 - **ReMedy International Research Agenda Unit,** Centre of New Technologies, University of Warsaw, 02-097 Warsaw, Poland*

Correspondence to Carlo Vascotto: Department of Medicine, University of Udine, 33100 Udine, Italy. *carlo.vascotto@uniud.it (C. Vascotto)*
https://doi.org/10.1016/j.jmb.2020.11.012
Edited by C. Kalodimos

Abstract

Mitochondria are essential cellular organelles that import the majority of proteins to sustain their function in cellular metabolism and homeostasis. Due to their role in oxidative phosphorylation, mitochondria are constantly affected by oxidative stress. Stability of mitochondrial DNA (mtDNA) is essential for mitochondrial physiology and cellular well-being and for this reasons mtDNA lesions have to be rapidly recognized and repaired. Base excision repair (BER) is the main pathway responsible for repair non-helix distorting base lesions both into the nucleus and in mitochondria. Apurinic/Apyrimidinic Endonuclease 1 (APE1) is a key component of BER pathway and the only protein that can recognize and process an abasic (AP) site. Comprehensions of the mechanisms regulating APE1 intracellular trafficking are still fragmentary. In this study we focused our attention on the mitochondrial form of APE1 protein and how oxidative stress induce its translocation to maintain mtDNA integrity. Our data proved that: (i) the rise of mitochondrial ROS determines a very rapid translocation of APE1 from the intermembrane space (IMS) into the matrix; and (ii) TIM23/PAM machinery complex is responsible for the matrix translocation of APE1. Moreover, our data support the hypothesis that the IMS, were the majority of APE1 resides, could represent a sort of storage site for the protein.

Introduction

Mitochondria are essential organelles with numerous functions in cellular metabolism and homeostasis. The most prominent role of mitochondria is to produce ATP through the oxidation of substrates in the presence of oxygen and the release of electrons from cofactors such as NADH and $FADH_2$.[1] In the process of shuttling electrons to oxygen through the electron transport chain (ETC), protein complexes I, III, and IV of the ETC pump protons out of the mitochondrial matrix across the inner mitochondrial membrane generating a proton gradient within the inner mitochondrial membrane that is used by the ATP synthase (complex V) to drive phosphorylation of ADP to ATP. Although very efficient, this process is associated to the so-called electron leakage: a physiological phenomenon occurring when electrons exit the ETC prior to the reduction of oxygen to water by cytochrome *c* oxidase, reacting instead with oxygen to form superoxide anion ($O_2^{\cdot-}$).[2] In

addition to the electron leak, pathological defects of mitochondria respiration are also causative of reactive oxygen species (ROS) overproduction.[3–8] Superoxide anion is a highly reactive ROS that can transfer its unpaired electron to lipids, proteins and nucleic acids inducing oxidative damage.[9] To cope with the production of ROS, cells developed superoxide-scavenging enzymes such as superoxide dismutase (SOD) that catalyses the dismutation of the superoxide radical into oxygen or hydrogen peroxide.[10] In parallel to ROS scavenging enzymes, cells also developed mechanisms to repair oxidative-induced damages. In the case of nucleic acids, the integrity of mitochondrial DNA (mtDNA) is maintained via the mitochondrial base excision repair (mtBER) pathway, the major DNA repair mechanism acting in mitochondria.[11] BER is the primary pathway responsible for repairing small non-helix-distorting DNA lesions such as oxidised and alkylated bases into both the nucleus and mitochondria. The first step of the mtBER is operated by a DNA glycosylase that recognize and remove the damaged base leaving an abasic (AP) site. Next, Apurinic/apyrimidinic endonuclease 1 (APE1) enzyme acts by hydrolysing the phosphodiester bond at the AP site and then the gap is filled by the action of a polymerase γ (Polγ) that incorporates the correct nucleotide. Finally, DNA ligase III seals the nick reconstituting the original genetic information.[11] APE1 is a monomeric protein composed by 318 amino acid residues and beside its endonuclease activity, it is also involved in gene regulation through a redox mechanism.[12] The first 33 residues at the N-terminal are unstructured, present the nuclear localization signal (NLS),[13] and are required for protein–protein and protein-DNA interaction.[14] The region spanning amino acids 36–127 is responsible for the redox activation of several transcriptional factors including NF-κB, p53, HIF-1α and others, for which APE1 facilitates their DNA binding via reduction of critical cysteine residues.[15] The C-terminal domain from amino acid 61–318 is responsible for the apurinic/apyrimidinic site cleavage activity.[16]

The great majority of mitochondrial proteins are encoded by nuclear DNA and then translated in the cytoplasm. Precursor proteins are imported into mitochondria by specialized machineries that decode structural signals in the amino acid sequence of precursors to properly distribute them into four mitochondrial compartments: outer membrane (OM), intermembrane space (IMS), inner membrane (IM), and matrix.[17] The translocase of the inner membrane (TIM23) complex represents the channel through which soluble proteins enter the matrix. The translocation requires engagement of the presequence translocase-associated motor (PAM) complex, which binds to the TIM23 complex and catalyses the translocation of the entire protein through TIM23, and it is dependent on ATP and membrane potential ($\Delta\Psi_m$).[17]

APE1′s localization is eminently nuclear although the protein is also present within the mitochondrial compartment.[18,19] APE1 does not carry a canonical mitochondrial targeting signal (MTS) and the nuclear and mitochondrial forms of the protein show the same electrophoretic mobility.[20] This exclude any possible proteolytic removal of the NLS to be responsible of the mitochondrial translocation. What is known about the mechanism driving APE1 into the mitochondrial compartment is that residues Lys299 and Arg301 are essential for the interaction with Tom20, a component of the mitochondrial outer membrane pore TOM.[21] Moreover, it has been proved that oxidative stress induces the accumulation of APE1 into the mitochondria.[22] Once passed the outer membrane, APE1 is bound by Mia40 becoming the substrate of the MIA pathway.[23] Typical substrates of the MIA pathway are small proteins, around 10 KDa, whose destination is the IMS. These proteins are cysteine enriched, belong to the families of the twin CX3C and CX9C proteins and fulfill different functions in the mitochondria.[24] However, in recent years non-canonical substrates of the MIA pathway that localize within the mitochondrial matrix have been described. The tumor suppressor protein p53 was found to localize within human mitochondria through the MIA pathway[25] and also the mitochondrial ribosome subunit Mrp10 was demonstrated to be oxidized by Mia40 during the import.[26] A few years ago we demonstrated that Mia40 is able to interact and bind APE1 by forming a disulfide bridge between APE1′s Cys93 and Mia40′s Cys55 residues.[23] Through sub-fractionation experiments, we also demonstrated that the majority of mitochondrial APE1 is present within the IMS, while a small fraction (around 20%) of mitochondrial APE1 (mtAPE1) localizes into the matrix where the mtDNA is located.[20] In this study we address, how oxidative stress induces a rapid translocation of APE1 from the IMS into the matrix to repair damaged mtDNA, and which is the IM channel through which APE1 enters the matrix.

Results

Mitochondrial oxidative stress induces IMS/matrix translocation of APE1 to preserve mtDNA integrity

Antimycin A (AMA) is an inhibitor of the mitochondrial electron transport chain complex III, which inhibition specifically induces mitochondrial oxidative stress.[27] To induce mitochondrial ROS generation, HeLa cells were treated for 30 min in absence of serum with 10, 25, and 50 μm of AMA. Then, ROS production was measured by FACS using the cell-permeant 2′,7′-dichlorodihydro fluorescein diacetate (H_2DCFDA) as an indicator for cellular ROS (Figure 1(A)). The dose of 25 μM resulted to be effective in generating ROS without

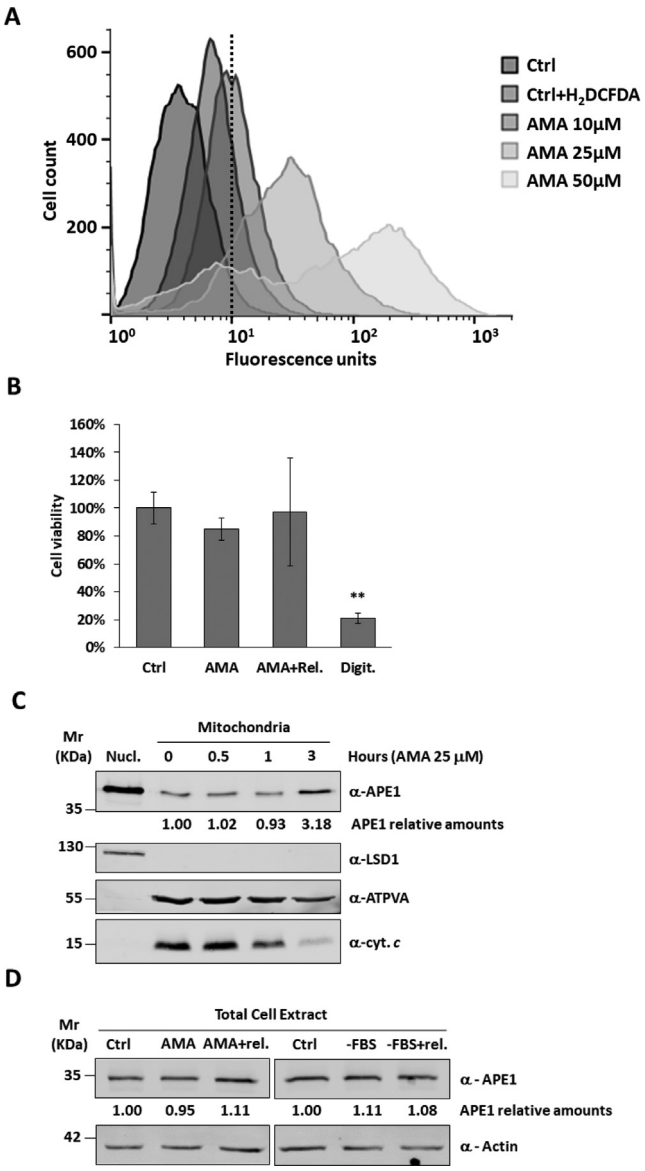

Figure 1. Antimycin treatment induces oxidative stress without altering cell viability nor the expression levels of APE1. (A) Flow cytometry analysis of HeLa cells treated with AMA. HeLa cells have been treated with 10 μM, 25 μM, and 50 μM of AMA for 30 min. Then, reactive oxygen species (ROS) production was measured by FACS using the cell-permeant 2′,7′-dichlorodihydrofluorescein diacetate (H_2DCFDA) as an indicator for cellular ROS. (B) MTS assay after AMA treatment confirmed that conditions used to induce mitochondrial oxidative stress do not affect viability. Digitonin was used as positive control. (C) Western blot of mitochondrial fractions after AMA treatment. HeLa cells were treated with 25 μM of AMA for the indicated times. 10 μg of nuclear fraction and 30 μg of mitochondria were analysed. After 30 min or 1 h of AMA treatment APE1 accumulation does not change significantly, however after 3 h the amount of APE1 translocated inside mitochondria is significantly higher. Cytochrome *c* is also affected by the treatment. (D) Western blot analysis of 15 μg of total cell extracts from HeLa cells treated with AMA (*left*) or in the absence of serum (*right*). In both cases, the analysis confirmed that APE1 expression levels are not affected by the experimental conditions used. Actin was use as loading control.

affecting cell viability (Figure 1(B)) and therefore was chose as treatment to verify if oxidative stress induces the variation of mitochondrial APE1 content. Cells were treated for 0.5, 1, and 3 h with 25 μM of AMA, then growth for an additional hour in the presence of complete media to reactivate cell metabolism. After harvesting, mitochondria were isolated, and mtAPE1 content evaluated by Western blot. As visible in Figure 1(C), the total amount of mtAPE1 does not change after 30 min or 1 h of treatment, while it is significantly increased after 3 h. In parallel, cytochrome *c* levels were monitored as indicator of mitochondrial integrity showing that 30 min exposure were able to induce

oxidative stress without leading to mitochondria permeabilization that in turn occurs for longer exposures. Because AMA treatment was performed in the absence of serum, we verified that total APE1 expression levels were not altered by 30 min of starvation followed by 1 h of release in the presence of serum (Figure 1(D), *right*), or by AMA treatment itself (Figure 1(D), *left*).

The majority of APE1 protein localizes into the nucleus, and therefore to quantify the expression levels and to study the intra-mitochondrial trafficking of mtAPE1 in all our experiments mitochondria and isolated mitoplasts were treated with proteinase K (PK) for 15 min at 4°C to degrade outside proteins. To evaluate the efficiency and quality of our isolation protocols and to asses APE1's proteolytic pattern, mitochondria were treated with PK for 15 min. With the exception of Tom20, which resided on the OM and resulted to be degraded by PK treatment, the intensity levels of all other markers were unaffected confirming that mitochondria are intact. Concerning APE1, the majority of the protein was protected from PK (Figure 2(A), *left*). Then, isolated mitochondria were resuspended in isotonic (SM buffer) or hypotonic (M buffer) sucrose solution and incubated on ice for 30 min. The hypotonic solution determined the swelling and consequent rupture of the outer mitochondrial membrane releasing IMS proteins. Then, PK was added for 15 min on ice and samples were analyzed on Western blot (Figure 2(A), *right*). As visible on the right panel, PK digestion of APE1 led to the cleavage of the first 33 residues at the N-terminal and the accumulation of a truncated form of the protein (NΔ33).[28] These experiments

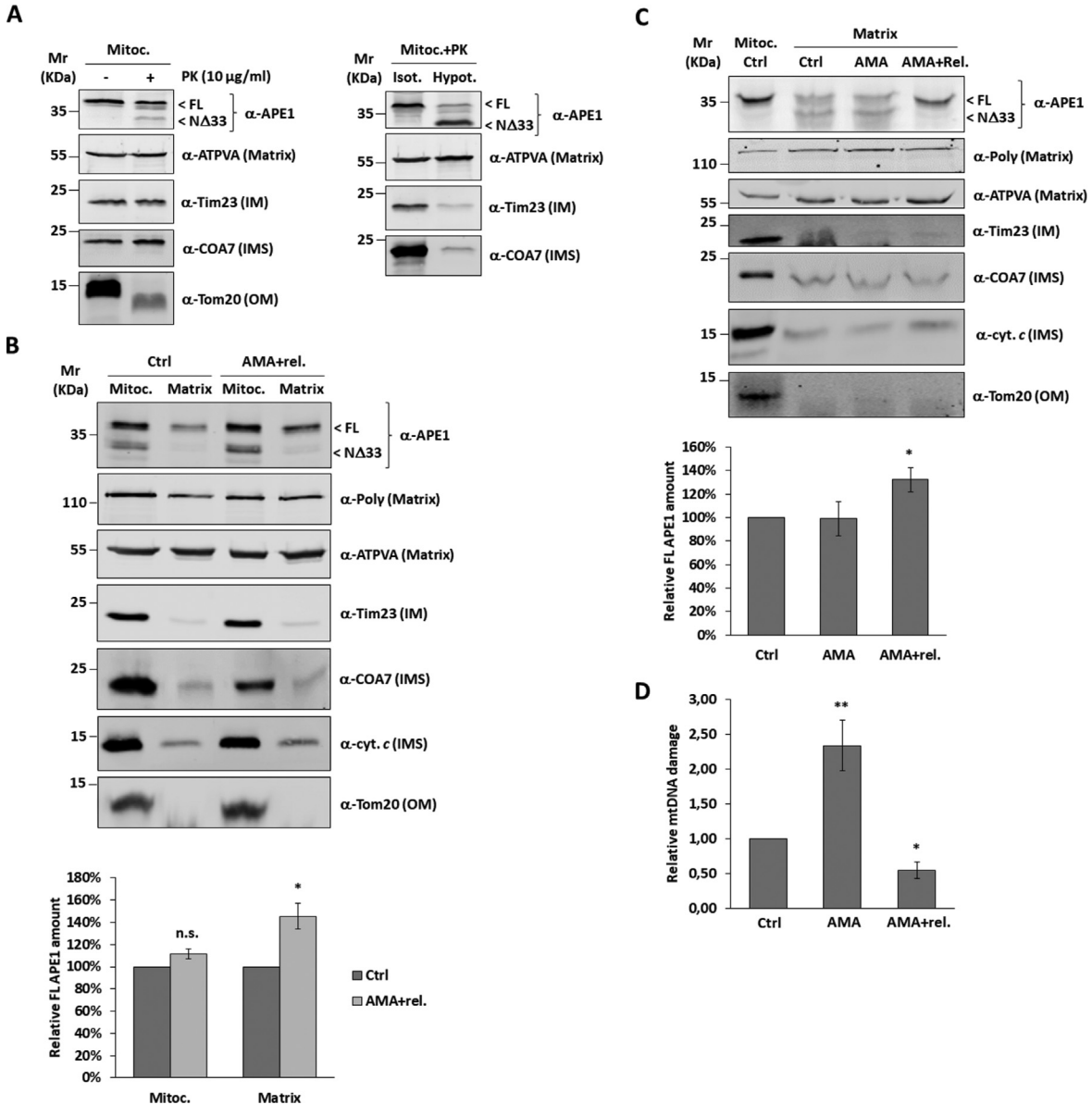

confirm the efficiency of our isolation procedures and that the quote of APE1 inside the mitochondria (*left panel*) or the matrix (*right panel*) is protected by PK digestion and is visible as a full-length (FL) form.

Having established the experimental conditions to induce mitochondrial ROS generation without affecting mitochondrial integrity and to specifically quantify the amount of mtAPE1, HeLa cells were treated for 30 min with 25 μM of AMA followed by one hour of release in the presence of 10% FBS. Then, mitochondria were isolated and sub fractionated by mitoplasting to quantify the quote of matrix APE1. While the total quantity of mtAPE1 does not change as consequence of ROS generation, a significant increase of the matrix APE1 (FL) content is visible. This reflects for an internal redistribution of mtAPE1 from IMS into the matrix (Figure 2(B)). The efficiency of PK treatment is confirmed by the digestion of Tim23 which is exposed to PK action after mitoplasting while absence of degradation of matrix proteins Polγ and ATPVA assure the intactness of mitoplasts. IMS protein COA7 was used to evaluate the homogeneity of mitochondrial swelling of control and AMA treated samples during mitoplasts preparation. Unaltered levels of cytochrome *c* confirmed the absence of membrane permeabilization during manipulation of isolated mitochondria. To exclude the possibility that the observed increase of APE1 into the matrix as consequence of oxidative stress could be ascribed to newly synthetized and/or cytoplasmic protein newly imported, isolated mitochondria were treated with PK to degrade all external protein and then treated for 30 min with 5 μM of AMA followed by 1 h or release. Matrix were isolated, followed by PK digestion, and analysed for the presence of APE1. In control (Ctrl) and AMA samples an NΔ33 APE1 form excluded from the matrix is visible. In respect to the experiment showed in Figure 2(B), this form is more represented. Possibly, treatment of isolated mitochondria with AMA for 30 min followed by one hour of release could have negatively affected protein solubility determining the presence of IMS proteins in the mitoplast fraction. In accordance with the previous result, after the release all mtAPE1 resulted protected from PK digestion meaning that the quote initially present in the IMS was translocated into the matrix as consequence of oxidative stress induction (Figure 2(C)). This experiment support our hypothesis that oxidative stress induces a rapid translocation of the IMS pull of APE1.

APE1 represents the main human endonuclease, an enzyme that can recognize and process an abasic (AP) site. The absence of APE1 determines the accumulation of damaged bases that are not processed by DNA glycosylases. Formamidopyrimidine DNA Glycosylase (Fpg) is a bifunctional DNA glycosylase and releases damaged purines generating an AP site which is further processed by its AP lyase activity creating

Figure 2. Oxidative stress induces IMS/matrix translocation of APE1. (A) PK proteolytic pattern of mitochondrial APE1. *Left*: 30 μg of mitochondria isolated from HeLa cells were treated or not with PK (10 μg/ml for 15 min at 4 °C) and then analyzed by Western blot. Only the OM marker Tom20 resulted degraded confirming the intactness of isolated mitochondria. *Right*: 30 μg of mitochondria isolated from HeLa cells were resuspended in isotonic or hypotonic sucrose buffer, treated with PK (10 μg/ml for 15 min at 4 °C) and then analyzed for the content of APE1. Protein inside the mitochondrial is protected by PK digestion and visible as a full-length (FL) form. On the contrary, protein outside is degraded at the N-terminal generating a truncated form (NΔ33). Degradation of Tim23 and COA7 by PK treatment confirmed the efficacy of the rupture of OM as consequence of swelling, while ATPVA confirmed that mitochondrial inner membranes were intact. (B) Mitochondrial subfractionation analysis of HeLa cells after AMA treatment. Representative Western blot analysis of mitochondrial and matrix fractions after 25 μM AMA treatment for 30 min (*top*). Isolated mitoplasts were treated with proteinase K (PK) for 15 min at 4℃ to degrade outside proteins. While total amount of APE1 does not change in the whole mitochondrial fraction, the full-length (FL) is significantly higher in the mitochondrial matrix obtained from AMA treated cells. ATPVA, Tim23, COA7, and Tom20 were used as subfractionation controls and mitoplasting efficiency for matrix, IM, IMS, and OM, respectively. In the graph (*bottom*) are reported the densitometric analysis of total mtAPE1 (Mitoc.) and the matrix quote (Matrix) normalized for Polγ. Data reported are the average ± SD of five independent biological replicates. (*: $p < 0.05$). (C) Western blot analysis of matrix obtained from isolated mitochondria after 5 μM AMA treatment for 30 min. Isolated mitoplasts were treated with proteinase K (PK) for 15 min at 4℃ to degrade outside proteins. After the release, all mtAPE1 is translocated into the matrix and visible as a full-length (FL) form. ATPVA, Tim23, COA7, and Tom20 were used as subfractionation controls and mitoplasting efficiency for matrix, IM, IMS, and OM, respectively. In the graph (*bottom*) are reported the densitometric analysis of the matrix quote of APE1 (FL) normalized for Polγ. Data reported are the average ± SD of three independent biological replicates. (*: $p < 0.05$). (D) mtDNA damage evaluation a in Hela cells after AMA treatment. mtDNA damage was evaluated from cells treated with 25 μM AMA for 30 min and cells treated for 30 min and allowed to recover for 1 h. After 30 min of AMA treatment levels of mtDNA damage were significantly increased, while after 1 h of release levels were lower than untreated cells. Data reported are the average ± SD of four independent biological replicates. (*: $p < 0.05$; **: $p < 0.01$).

a one nucleotide DNA gap with 5′ and 3′ phosphate termini. By performing a long-range PCR using a high-fidelity DNA polymerase, which action is inhibited by presence of the DNA gap generated by Fpg, we quantified the relative levels of mtDNA damage in control and AMA treated HeLa cells. As expected, induction of mitochondrial ROS production by AMA treatment led to a significantly increased level of mtDNA damage (2.34 fold ± 0.36). In agreement with the biochemical analyses showing the accumulation of APE1 into the matrix after 1 h of release, the levels of mtDNA damage resulted lower than that of untreated control cells (0.55 fold ± 0.12) (Figure 2(D)).

In conclusion, our experiments prove that oxidative stress induces a rapid translocation of mtAPE1 from the IMS into the matrix as a protective mechanism for maintaining mtDNA stability.

APE1 interacts with TIM23 and PAM motor complexes

Upon translocation through the TOM pore, soluble matrix proteins carrying a pre-sequence are handed over to the TIM23 complex to pass the IM and entering the matrix. Although APE1 does not possess any mitochondrial pre-sequence, we assessed if its IMS/matrix translocation occurred through TIM23 and its associated motor complex PAM (Figure 3(A)). For this purpose, we performed *in organello* import experiment by using *in vitro* expressed APE1-HisTag protein and intact mitochondria isolated from HEK293 cells. Recombinant APE1 and mitochondria were incubated at 37 °C for 30 min, treated with PK to degrade protein not imported, and finally lysed under native conditions to preserve protein/protein interaction. Input, eluate, and unbound fractions from control (Mock) and APE1-HisTag affinity purified (AfP) samples were separated onto SDS-PAGE and analysed by Western blotting. As visible in Figure 3(B), in the eluate of the AfP fraction Tim23 and the two protein of the PAM complex, mtHSP70 and DNAJc19, resulted enriched respect to the control (Mock). To support the specificity of the binding between the bait (APE1-HisTag) and the channel proteins we evaluated the presence of Tim29, a component of the IM channel TIM22, two IM proteins (Mic60 and AIF), and that of the OM protein Sam50 (Figure 3(B)). All these proteins were absent in the eluate supporting the specificity of the interaction between APE1 and the import complex TIM23/PAM. Next, by using specific siRNA we reduced Tim23 expression and evaluated the levels of mtAPE1 into the matrix. Accordingly with our hypothesis, the silencing of Tim23 protein determined a significant reduction in the quote of APE1 into the matrix (Figure 3(C)). As positive control of our experiment we evaluated the levels of MnSOD, a protein which is imported into the matrix through the TIM23/PAM complex.[29] As for APE1, also the levels of matrix MnSOD resulted reduced by silencing of Tim23.

We proved that APE1 translocation from IMS into the matrix occurs rapidly upon induction of mitochondrial oxidative stress (Figure 2(B) and (C)). To further support our biochemical data, we decided to measure the kinetics of interaction between APE1 and the PAM protein DNAJc19 by using Proximity Ligase Assay (PLA) technology. DNAJc19 has a transmembrane segment and exposes four residues of the N-terminus to the IMS side of the IM while the majority of the protein is located in the matrix side and therefore its interaction with APE1 could occur only during its passage through TIM23 (Figure 3(A)). Under basal conditions an average of 22 ± 6 interaction per cells were detected. Mitochondrial ROS formation by AMA treatment determined an increased number of interactions after 20 min of treatment (33 ± 7), with a peak at 30 min with 55 ± 15 PLA dots/cell. By removing the stimulus, the number of interactions decreases to the basal levels (Figure 3(D)). A representative image showing all time points analysed is visible in Supplementary Figure S1. This data confirms the role of the TIM23/PAM complex in the matrix translocation APE1. Moreover, this further proves that ROS production triggers a rapid redistribution of mtAPE1 from the IMS into the matrix as a mechanism to preserve mitochondrial genome stability.

Selective TIM23 inhibition blocks APE1 trafficking preventing mtDNA repair

In 2017, Filipuzzi *at al.* described stendomycin as a potent and specific inhibitor of the TIM23 complex in yeast and mammalian cells.[30] To corroborate our findings, we treated HeLa cells for 24 h with stendomycin and then measured the interaction between APE1 and DNAJc19 by performing PLA analysis. As visible, the treatment almost completely abolishes the number of dots per cell, reducing their number from 23 ± 7 in the control to 4 ± 2 in treated cells (Figure 4(A), Supplementary Figure S2). To rule out any effect ascribable to mitochondrial membrane potential HeLa cells were treated for 24 h with stendomycin at the final concentration of 500 nM and then cells were stained with MitoTracker red. We did not observe any loss of MMP which would also block protein import supporting the specificity of the inhibitory effect observed (Supplementary Figure S3).

Next, we measured if inhibition of TIM23 by stendomycin treatment affected the repair of mtDNA after oxidative stress damage. For this purpose, HeLa cells pre-treated for 24 h with stendomycin (Stendo) and control cells (Ctrl) were treated for 30 min with 25 μM AMA and then growth for an additional hour. As previously

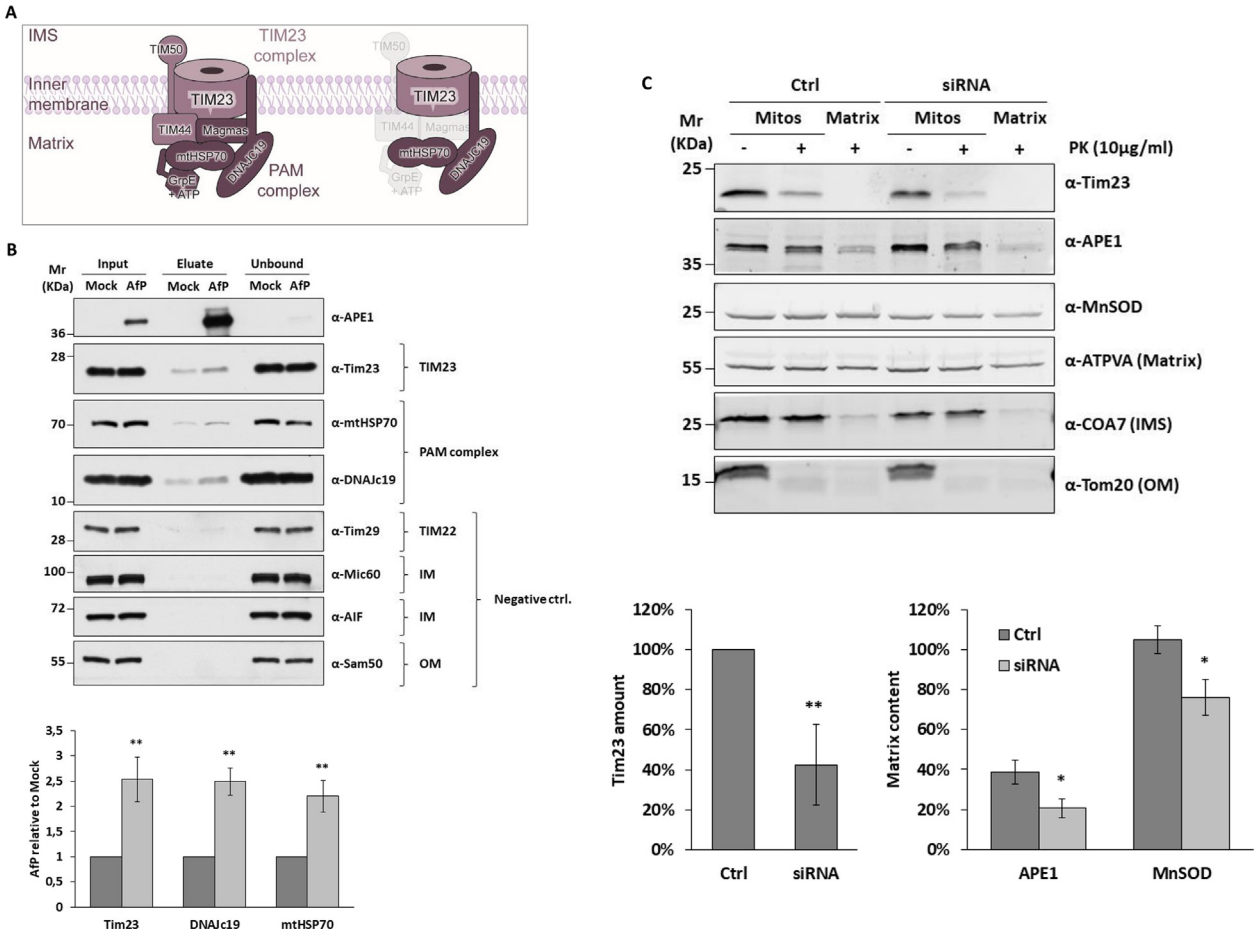

Figure 3. APE1 interacts with TIM23/PAM complex. (A) Schematic representation of TIM23/PAM complex. On the left side of the image the principal components of TIM23 and PAM are s reported. On the right side, proteins found in the affinity purification experiments to interact with APE1 have been highlighted. (B) Western blot (*top*) and relative quantification (*bottom*) of the affinity purification analysis of APE1 imported *in organello* in mitochondria. After *in organello* import, control sample (Mock) and APE1-HisTag (AfP) were purified under native conditions from isolated mitochondria, separated on 12% SDS-PAGE, and analysed by Western blot to evaluate the interaction with TIM23/PAM complex proteins. Tim23 and the two components of the PAM complex (mtHSP70 and DNAJc19) resulted enriched in the AfP fraction. Tim29, Mic60, AIF and Sam50 were used as negative control to support the specificity of the binding with the TIM23/PAM complex proteins. Data reported are the average ± SD of four independent biological replicates. (**: $p < 0.01$). (C) Western blot analysis (*top*) of mitochondrial extracts of Tim23 transiently silenced HeLa cells. Loss of Tim23 negatively affects APE1 import into the mitochondrial matrix. Also, the matrix levels of MnSOD, are reduced by the silencing of Tim23. ATPVA, COA7 and Tom20 were used as subfractionation control for matrix, intermembrane space and outer membrane, respectively. Graphs on the bottom show the expression levels of Tim23 in siRNA cells (*left*) and the percentage of matrix APE1 and MnSOD in control and siRNA cells respect to the total protein present in mitochondria after PK treatment (*right*). Data reported are the average ± SD of four independent biological replicates. (*: $p < 0.05$; **: $p < 0.01$). (D) Representative immunofluorescence images (*top*) and relative box and whisker plot (*bottom*) of PLA analysis between APE1 and DNAJc19 in cells treated with AMA. Data reported in the plot accounted for the average number of PLA signals of at least 35 randomly selected cells per condition. The plot shows the analysis on cell treated with AMA for 10 and 20 min, 30 min, and after 30 and 60 min of release. Nuclei were stained with DAPI, while PLA signal is visible as red dots. White bar corresponded to 10 μm. Similar images were obtained in other two independent experiments. Statistical significance was calculated *versus* untreated cells. (n.s.: not significant; *: $p < 0.05$; **: $p < 0.01$).

reported in Figure 2(D), AMA treatment determines a significant increase in the levels of mtDNA damage which is rescued after the release. On the contrary, cells pre-treated with stendomycin showed slightly increased, even if not significant ($p < 0.054$), basal level of mtDNA damage (1.36 ± 0.23) that could be associated to the mitochondrial stress induced by the inhibition of TIM23 determined by 24 h stendomycin treatment. The short treatment with AMA is not effective in

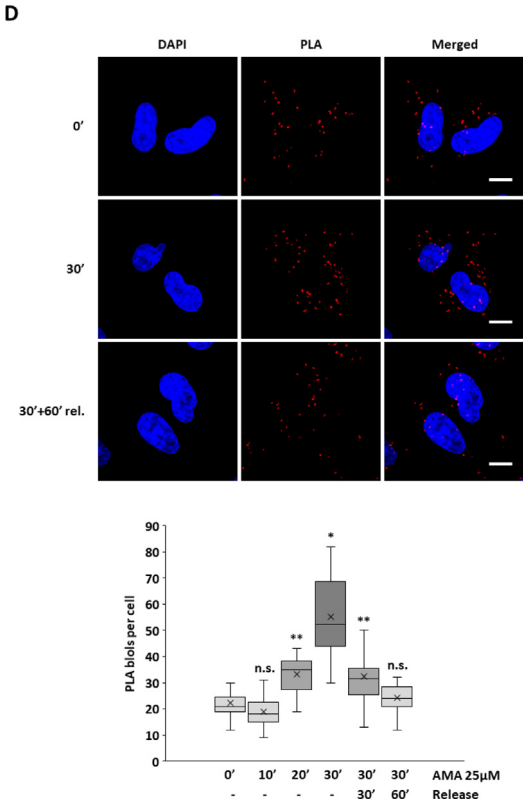

Fig 3. *(continued)*

inducing any rise in the levels of mtDNA damage (1.19 ± 0.27). This could be explained considering that pre-treatment with stendomycin induces mitochondrial stress triggering an adaptive response by enhancing repair mechanisms.[31–34] Interestingly, differently from the control cells where mtDNA lesions after AMA treatment were lower than that untreated sample (0.47 ± 0.14), we did not observe the reduction of mtDNA damage levels above the control upon release (1.21 ± 0.27) confirming that inhibition of TIM23 prevent the IMS/matrix translocation of mtAPE1 (Figure 4(B)).

Discussion

APE1 is the main human endonuclease and can recognize and process AP sites present into both the nuclear and mitochondrial genome. The importance of the APE1 protein in maintaining cell homeostasis by playing a major role in the BER pathway and by such preserving the intactness of DNA, has been broadly discussed.[12,35,36] However, up until recently the main focus was given to the nuclear fraction of APE1, despite of the fact that the protein has been known to localize also in the mitochondrial compartment. Information about APE1′s subcellular trafficking is still scanty and incomplete. Data published by Li *et al.* demonstrated that APE1 residues Lys299 and Arg301 are essential for the interaction with the component of the TOM pore.[21] After passing the outer membrane APE1 becomes the substrate of Mia40 and is released in a partially folded state into the IMS.[23] Mitochondrial sub fractionation analyses revealed an uneven distribution of APE1 within the IMS space and matrix. Although the mtDNA and all mtBER enzymes are present within the matrix, unexpectedly the majority of APE1 resides into the IMS (Figure 2(B)).[20]

Initially, we seated up experimental conditions to induce APE1′s IMS/matrix translocation without altering the total amount of APE1 present within the mitochondria by using AMA.

Sub-fractionation experiments of cells and isolated mitochondria treated with AMA revealed that oxidative stress increases the quote of APE1 into the matrix (Figure 2(B) and (C)). In agreement with the biochemical analysis the levels of mtDNA damage resulted lower than that of untreated control cells (Figure 2(D)). Considering that APE1 is the major human apurinic/apyrimidinic endonuclease, such decrease in the number of mtDNA lesions could be ascribed mainly to increased amount of APE1 into the matrix. Our experiments proved that oxidative stress induces a rapid translocation of mtAPE1 from the IMS into the matrix as a protective mechanism for maintaining mtDNA stability. Moreover, our data suggest that the recruitment of mtAPE1 upon induction of oxidative stress follows a biphasic model: an initial very rapid response where the protein retained in the IMS is moved into the matrix. In the event of a persistent oxidative stress condition, new protein is synthetized and then translocated into the mitochondria. In this scenario, the accumulation of APE1 in the IMS could represent a storage site for the protein that in case of need could be rapidly moved into the matrix.

Having establish that oxidative damage to mitochondrial DNA triggers a rapid response and the accumulation of APE1 into the matrix, the next step was to determine the IM channel through which APE1 enters the matrix. Interaction between a precursor protein and its transport channel is by nature limited in time and strength and therefore very difficult to observe and analyse. To overcome this problem APE1-HisTag protein was synthetized *in vitro* using wheat germ system and then imported into isolated mitochondria of HEK293 cells. Respect to a cellular system that is characterized by an equilibrium state, the *in organello* protein import system used is characterized by a continuous import of the precursor protein. This maximize the length of the interaction between the pore and the incoming protein facilitating the detection of channel components within the eluate. Therefore, taking advantage of a C-terminal His-tag, APE1 was purified under native condition to preserve protein/protein interaction and eluates were

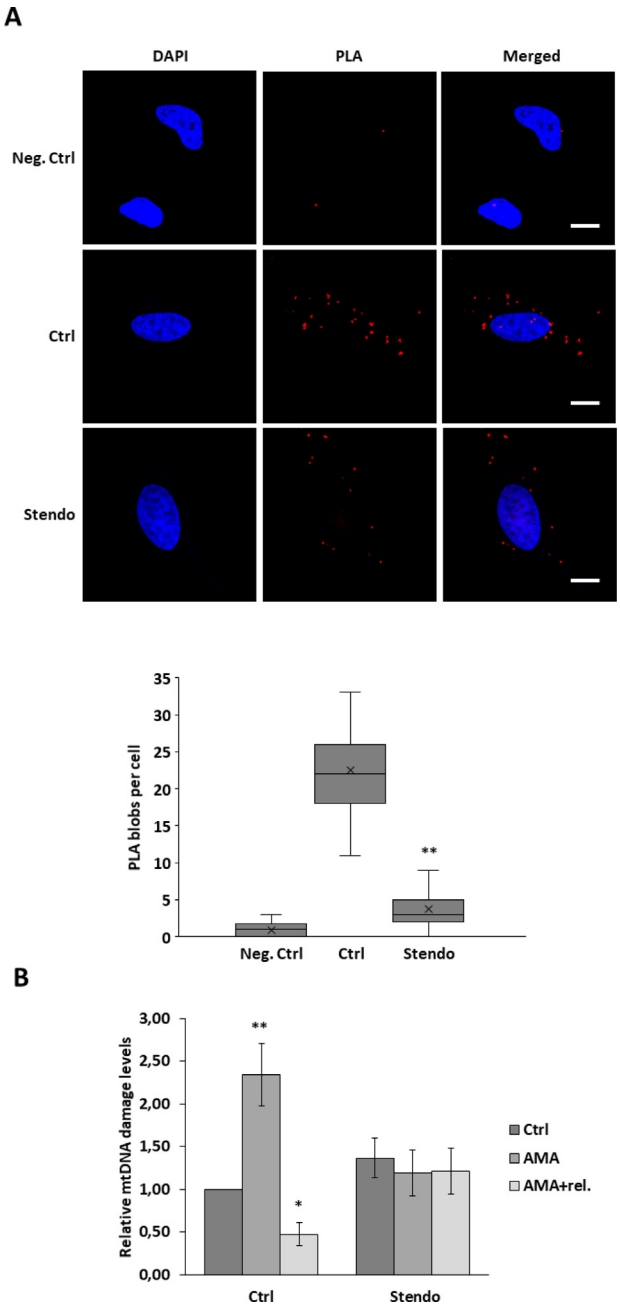

Figure 4. Specific inhibition of TIM23 by stendomycin prevent APE1′s translocation into the matrix. (A) Representative immunofluorescence images (*top*) and relative box and whisker plot (*bottom*) of PLA analysis between APE1 and DNAJc19 in cells treated with stendomycin. HeLa cells were treated for 24 h with 500 nM stendomycin treatment for 24 h to block TIM23 channel. APE1-DNAJc19 interaction was measured via PLA analysis. In the control cells, no stendomycin was added to the cultured cells, while negative control reaction was carried out omitting anti-DNAJc19 antibody. Nuclei were stained with DAPI, while PLA signal is visible as red dots. White bars correspond to 10 μm. Similar images were obtained in other two independent experiments. Data reported in the histogram accounted for the average number of PLA signals of at least 35 randomly selected cells per condition. Statistical significance of stendomycin effect on APE1-DNAJc19 interaction was calculated *versus* untreated cells. (**: $p < 0.01$). (B) mtDNA damage evaluation in Hela cells treated with stendomycin. mtDNA damage was evaluated in cells treated or untreated with 500 nM stendomycin for 24 h where oxidative stress was induced with 30 min AMA treatment (AMA) followed by 1 h of release (AMA + rel.). HeLa cells treated only with AMA show an increased level of mtDNA damage, which is completely rescued after 1 h of release. In stendomycin treated cells mtDNA damage levels are unchanged, even in the presence of the oxidative stress caused by the AMA treatment. Data reported are the average ± SD of three independent biological replicates. (*: $p < 0.05$; **: $p < 0.01$).

analysed by Western blot. The presence of Tim23 and of two components of the PAM motor complex, mtHSP70 and DNAJc19, suggested that the translocation of APE1 from the IMS into the matric does occur through TIM23 complex (Figure 3(B)). To validate this hypothesis, we used two orthogonal approaches to block TIM23: the silencing of Tim23 and the use of TIM23 specific inhibitor stendomycin. In the first case we observed a significant reduction in the amount of matrix APE1 determined by the silencing of Tim23 (Figure 3(C)). Accordingly, the inhibition of the channel by stendomycin prevented the translocation of APE1 that was evaluated in terms of interactions with the PAM protein component DNAJc19 (Figure 4(A)). The analysis of the kinetic of interaction between APE1 and DNAJc19 confirmed that APE1′s IMS/matrix translocation occurs rapidly upon induction of oxidative stress (Figure 3(D)).

The interests of the scientific community involved in the study of the cellular mechanisms responsible for the maintenance of genomic stability have been mainly focused on the nuclear DNA. APE1 is an essential factor in cellular processes such as genome stability and gene expression regulation. Its importance in maintaining cell homeostasis by playing a major role in the BER pathway and thereby preserving the integrity of nuclear DNA has been broadly discussed.[12,35,37] However, APE1 and the BER pathway are also present in mitochondria. Stability of mtDNA is essential for mitochondrial metabolism and the functioning of the respiratory chain and this explain the growing interest in the mitochondrial nature of DNA repair proteins. To our knowledge, this study represents the first attempt to investigate the molecular mechanisms involved in the sub-mitochondrial trafficking dynamic of APE1 (Figure 5). In our previous works we proved that after entering the IMS and becoming the substrate of the MIA pathway, APE1 is released into the IMS.[18,20] We also reported that the majority of APE1 was unexpectedly present into the IMS but at that time we did not have a biological explanation for this. Moreover, also how the protein was further translocated into the matrix was still an open question. With this research we fulfilled this gap proving that the TIM23/PAM complex is responsible for the matrix internalization of APE1. Moreover, we demonstrated that oxidative damage to mtDNA triggers a rapid translocation response inducing the translocation of APE1 from the IMS into the matrix. We hypothesize that retention of APE1 into the IMS could represent a sort of storage site and that the protein could be associated to small IMS chaperons. In this scenario, the rise of ROS levels can alter this equilibrium inducing the dissociation of APE1 and its translocation into the matrix. However, further studies are required in order to verify this hypothesis. A second and maybe more relevant question that still require an answer is how APE1 is targeted into the nucleus rather than in mitochondria. Although APE1 possesses an NLS at the N-terminal, both the nuclear and mitochondrial forms are full length and this exclude the proteolytical removal of the N-terminal as the mechanism to direct the protein into the mitochondria. Our data proved that mitochondrial oxidative stress initially determined a rapid IMS/matrix translocation of APE1 without any contribution of newly synthetized protein. However, by prolonging the stimulus the total amount of APE1 into the mitochondria increased. A possible explanation is that oxidative stress determines still unidentified PTMs responsible for directing newly synthetized APE1 into the mitochondria. A different scenario could foresee the involvement of interacting proteins and a modification of APE1 interactome in response to cell stimuli as a way for conveying the protein into the nucleus or mitochondria.

Many studies have shown that APE1 is overexpressed in a variety of cancers, suggesting a possible prognostic significance and therapeutic target for this protein. Understanding the molecular mechanisms responsible for the intracellular trafficking of APE1 could led at the development of innovative strategy for anticancer treatment based on interfering with APE1 translocation.

Material and Methods

Cell culture and treatments

HeLa and HEK293 cells were grown at 37 °C with 5% CO_2 in DMEM (Dulbecco's modified Eagle's medium), supplemented with 10% fetal bovine serum (FBS), 100 U/mL penicillin and 10 μg/mL streptomycin. For Antimycin treatments, where not otherwise specified, cells were treated for 30 min with 25 μM Antimycin A (AMA) in DMEM without serum; release was performed for the indicated time in DMEM supplemented with FBS. AMA treatment of isolated mitochondria was performed on MIB buffer without serum with 5 μM of AMA for 30 min, then mitochondria were resuspended for an additional hour in MIB. Stendomycin was used on HeLa cells at the final concentration of 500 nM for 24 h in DMEM supplemented with 10% FBS.[30]

Cell viability assay

Cell viability upon AMA treatment was performed using CellTiter 96 AQueous One Solution Cell Proliferation Assay (Promega) in a 96 well plate. The day before the experiment, 10^4 HeLa cells/well were plated. 25 μM AMA was resuspended in DMEM without serum and cells were incubated for 30 min (AMA) or for 30 min followed by 1 h of release in DMEM complemented with 10% FBS

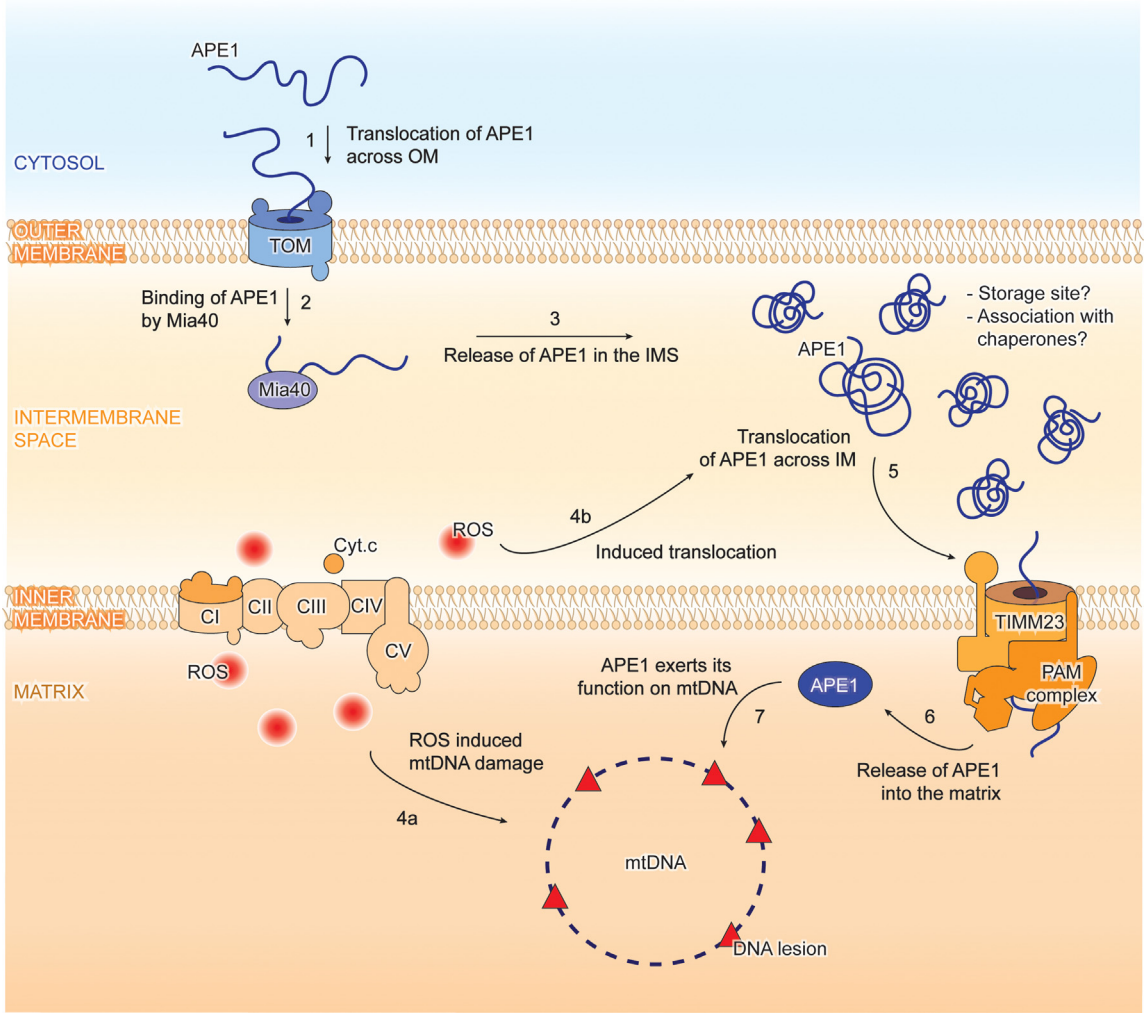

Figure 5. Model describing mitochondrial trafficking of APE1. When APE1 is translocated into the IMS of mitochondria through the TOM channel (1), it is bound by Mia40 (2), and then released in the IMS in a partially folded state (3). Here the protein is retained, possibly associated with chaperons, representing a sort of storage site. An excess of ROS generation determines mtDNA damage (4a) and consequently a yet-to-be-defined signal (4b) leads to the translocation of APE1 across the IM through the TIM23/PAM complex (5). Once released in the matrix (6), APE1 exerts its enzymatic activity on damaged mtDNA (7).

(AMA + rel.). DMEM without serum was used as control. As a positive control cells were incubated with 200 μg/mL of digitonin for 15 min.

After treatment, 20 μl of CellTiter 96 AQueous One Solution were added to 100 μl of DMEM and cells were incubated at 37 °C, 5% CO_2 for 1 h. Absorbance was measured at 490 nm using the EnSpire Multimode Plate Reader (PerkinElmer).

ROS measurement

To measure intracellular ROS production, $3x10^5$ cells were plated in a 6 wells multiwell. The day after, cells were treated with 5 μM of cell-permeant 2′,7′-dichlorodihydrofluorescein diacetate (H_2DCFDA) as an indicator for cellular ROS for 30 min in DMEM without serum and then the indicated amounts of Antimycin A were added to the medium for 30 min. An untreated control (Ctrl) was added as well as a background control only treated with H_2DCFDA (Ctrl + H_2DCFDA). Cells were washed in PBS, harvested and centrifuged at 250*g* for 4 min at 4 °C. All samples were resuspended in 300 μl of PBS and analysed at the cytofluorimeter FACScalibur (BD Biosciences) with excitation/emission wavelengths of 500 nm/520 nm. Ctrl + H_2DCFDA sample was considered as reference threshold.

Silencing of Tim23

One day before transfection cells were seeded in 150 cm plates at the density of 15×10^6 cells/plate. Cells were then transfected with 25 nM of either control (Ctrl) (Sense: AUGAGGUCAGCAUGGUC UG[dT][dT]; Anti-sense: CAGACCAUGCUGACCU

CAU[dT][dT]) or Tim23 siRNA (siRNA) (Sense: UAAAUAAGGAGACAGAGGG[dT][dT]; Antisense: CCCUCUGUCUCCUUAUUUA[dT][dT]) per plate using RiboJuice (Millipore) according to the manufacturer's instructions. After 24 h cells medium was replaced by low-glucose medium for 24 h and then by galactose medium for 24 h.

Preparation of total protein extracts and subcellular fractions

To prepare total cell extracts, HeLa cell were harvested by trypsinization and centrifuged at 250*g* for 5 min at 4 °C. Pellet was washed with cold PBS and resuspended in Lysis buffer [50 mM Tris-HCl pH 7.5, 150 mM NaCl, 1 mM EDTA, 1% (vol/vol) Triton X-100, protease inhibitor cocktail (Sigma), 0.5 mM PMSF] at a cell density of 10^7 cells/mL, incubated on ice for 30 min, and centrifuged at 20.000*g* for 20 min at 4 °C. Surnatant was collected and quantified by Bradford assay. To prepare subcellular fractions, cells were scraped in PBS, collected, and centrifuged at 250*g* for 4 min at 4 °C. The pellet was suspended in Mitochondrial Isolation Buffer (MIB) [20 mM HEPES pH 7.6, 1 mM EDTA, 220 mM Mannitol, 70 mM Sucrose] supplemented with 2 mg/mL Bovine Serum Albumin (BSA) and 2 mM PMSF, at a cell density of 8 ml MIB per gram of cells. Cells were mechanically broken using a 7 mL dounce homogenizer (Wheaton), centrifuged at 650*g* for 5 min at 4 °C. The pellet was conserved to prepare nuclear subfraction. Supernatant collected was centrifuged at 14,000*g* for 15 min at 4 °C. Pellet was washed with MIB supplemented with 2 mg/mL BSA, 1 M KCl and 2 mM PMSF, and centrifuged as before. A last wash was performed using MIB without BSA, and then mitochondria were resuspended in MIB. In parallel, nuclei were washed twice in T1 solution [10 mM HEPES pH 7.9, 10 mM KCl, 0.1 mM MgCl2, 0.1 mM EDTA70, 2 mM PMSF] and centrifuged at 1000*g* for 15 min at 4 °C. Nuclei were resuspended in T2 lysis buffer [20 mM HEPES pH 7.9, 420 mM NaCl, 1.5 mM MgCl2, 0.1 mM EDTA70, 5% glycerol, 2 mM PMSF]. Samples were incubated on ice for 20 min and centrifuged at 20,000*g* for 20 min at 4 °C. Supernatant was collected as nuclear protein fraction. Protein concentration was determined using Bio-Rad protein assay reagent (Bio-Rad). Subfractions purity was evaluated by Western blot analysis using LSD1 and ATPVA as nuclear and mitochondria markers, respectively, to exclude the presence of cross contaminations between the two organelles.

Preparation of mitoplasts

For the preparation of mitoplasts fractions, isolated mitochondria were pre-treated with PK at a final concentration of 10 μg/μl for 15 min at 4 °C to degrade all proteins outside mitochondria. Then, PK digestion was stopped with 2 mM PMSF. 90 μg of mitochondria were resuspended in hypotonic M buffer [20 mM HEPES (pH 7.4), 5 mM sucrose], while sample for whole mitochondria preparation were resuspended in isotonic SM buffer [20 mM HEPES (pH 7.4), 250 mM sucrose]. After 30 min incubation on ice, PK was added to all samples. Finally, 300 mM KCl was added to mitoplasts and then all the samples were centrifuged at 20,000*g* for 10 min at 4 °C. Pellets were resuspended directly in Leammli buffer for Western Blot analysis.

Western blot analysis

The reported amount of nuclear or mitochondrial protein subfractions were separated onto 12% SDS-PAGE. Then, proteins were transferred into a nitrocellulose membrane (Sartourius Stedim Biotech S.A.). Saturation of the membranes was performed for 1 h at room temperature using 5% non-fat dry milk in TBS-T [1XTBS supplemented with 0.1% Tween 20], followed by primary antibody incubation overnight at 4 °C [anti-APE1: 1:1000 monoclonal (Novusbio); anti-ATPVA: 1:2000 monoclonal (Abcam); anti-LSD1: 1:10000 polyclonal (Abcam); anti-cyt.*c*: 1:1000 polyclonal (Abcam); anti-Polγ 1:000 polyclonal (Abcam); anti-Tim23: 1:1000 polyclonal (Abcam); anti-mtHSP70: 1:1000 polyclonal (Enzo Life Sciences); anti-DNAJc19: 1:1000 (Abcam); anti-Tim29: 1:500 polyclonal (ProteinTech); anti-Mic60: 1:1000 (Abcam); anti-Sam50: 1:500 (costum prepared); anti-AIF: 1:200 polyclonal (abcam); anti-MnSOD: 1:000 monoclonal (Abcam); anti-COA7: 1:1000 polyclonal (Atlas antibodies HPA); anti-Tom20: 1:1000 polyclonal (Abcam)]. Membranes were washed three times for 5 min with TBS-T, incubated for 2 h with the secondary antibody, and washed again for three times. The signal was detected with the Odyssey CLx scanner (Li-Cor Bioscience) and densitometric analysis was performed with ImageStudio software (Li-Cor Bioscience). Images reported in Figure 3(B) were acquired through autoradiography using horseradish peroxidase conjugated secondary antibodies.

DNA extraction and mtDNA damage analysis

DNA was extracted using Qiagen genomic-tip 20/G and following manufacturer's indications. After isolation DNA was precipitated overnight with isopropanol, and then 10 μg were digested with Formamidopyrimidine DNA Glycosylase (Fpg) enzyme at 37 °C for 30 min. Fpg is a bifunctional DNA glycosylase with DNA N-glycosylase and AP lyase activities N-glycosylase activity. The enzyme releases damaged purines, including

FapyG and 8oxoG, generating an AP site. The AP lyase activity cleaves an AP site, via β and δ-elimination, creating a one nucleotide DNA gap with 5′ and 3′ phosphate termini. Fpg was inactivated at 60 °C for 10 min and DNA was precipitated overnight, resuspended in 50 μl of Tris-EDTA buffer pH 8.0. Quantification was determined with Quant-iT™ PicoGreen™ dsDNA Reagent (Invitrogen), according to manufacturer's instructions and DNA concentration was adjusted to 3 ng/μl.

mtDNA lesions were quantified by Q-PCR, using the following primers: Mitolong Forward: 5′-TCT AAG CCT CCT TAT TCG AGC CGA-3′ and Mitolong Reverse: 5′-TTT CAT CAT GCG GAG ATG TTG GAT GG-3′ which amplified an 8.9 Kbp mitochondrial fragment; Mitoshort Forward: 5-CCC CAC AAA CCC CAT TAC TAA ACC CA-3′ and Mitoshort Reverse: 5′-TTT CAT CAT GCG GAG ATG TTG GAT GG-3′ which amplified a 221 bp mitochondrial fragment. DNA was amplified with Platinum™ SuperFi™ DNA Polymerase (Invitrogen) using the following protocol: 2 min at 94 °C, 18 cycles of denaturation for 15 s at 94 °C, annealing for 10 s at 66 °C, extension for 5.30 min at 68 °C for the 8.9 Kbp fragment or annealing 45 s at 60 °C and extension for 45 s at 72 °C for the 221 bp fragment. A final extension for 10 min at 68 or 72 °C was performed for each fragment. To ensure quantitative conditions a sample with the 50% of template amount was included in each amplification and, as negative control, a sample without the template was used. PCR products were quantified in triplicate by using Quant-iT™ PicoGreen™ dsDNA Reagent (Invitrogen). The Mitoshort fragment was used to calculate the relative amount of mtDNA copies and to normalize the lesion frequencies calculated with the Mitolong fragment.[38]

In vitro APE1-HisTag expression

Human APE1′s cDNA was subcloned into pTNT vector (Promega), a 10xHisTag was added at the C-terminal and the construct was sequenced. Then, the cell-free Wheat Germ System (Biotechrabbit) was used for expressing APE1-HisTag. Briefly, Feeding solution [feeding mix 900 μl, amino acids 80 μl, Methionine 20 μl] and Reaction solution [reaction mix 15 μl, amino acids 4 μl, Methionine 1 μl, Wheat Germ lysate 15 μl, pTNT-APE1-HisTag vector 3 μg] were prepared as reported by manufacturer. Feeding and Reaction solutions were pipetted into the microplate, covered with adhesive film, and incubated at 24 °C for 24 h, shaking speed of 900 rpm. Fifty μl of recombinant APE1-HisTag protein has been recovered, evaluated on SDS-PAGE gel and used for *in organello* protein import on isolated mitochondria.

Isolation of mitochondria from HEK293 cells and in organello import of APE1-HisTag

A total of 9×10^6 HEK293 cells were seeded and grown in low-glucose medium for 24 h and then in galactose medium for 24 h. Cells were harvested, and mitochondria isolated as mentioned above. APE1-HisTag and control (empty vector/mock) proteins were synthesized *in vitro* using wheat germ system and imported into the isolated mitochondria of HEK293 cells. HEK293 were harvested and resuspended in ice-cold isotonic buffer [10 mM MOPS pH 7.2, 75 mM mannitol, 225 mM sucrose, and 1 mM EGTA] supplemented with 2 mg/ml BSA and 2 mM PMSF, and subjected to centrifugation at 1000*g* for 5 min at 4 °C. The cell pellet was then resuspended in cold hypotonic buffer [10 mM MOPS pH 7.2, 100 mM sucrose, and 1 mM EGTA] and incubated on ice for 7 min. The cell suspension was homogenized in a Dounce glass homogenizer (Sartorius). Cold hypertonic buffer [1.25 M sucrose, 10 mM MOPS pH 7.2] was added to the cell homogenate (1.1 ml per gram of cells). The homogenate was subjected to centrifugation at 1000*g* for 10 min at 4 °C to pellet the cellular debris. The supernatant containing mitochondria was then carefully removed and centrifuged again. The supernatant was then subjected to high speed centrifugation at 10,000*g* for 10 min at 4 °C to isolate mitochondria. The pellet was resuspended in isotonic buffer without BSA and quantified using the Bradford assay.

One mg of isolated mitochondria were suspended in 1 ml of Import buffer [250 mM sucrose, 80 mM potassium acetate, 5 mM magnesium acetate, 5 mM methionine, 10 mM sodium succinate, 20 mM HEPES/KOH pH 7.4] and incubated with 50 μl (5% v/v) of the *in vitro* synthetized APE1-HisTag protein at 37 °C for 30 min. Then, samples were treated with PK at the final concentration of 25 μg/ml for 15 min on ice to degrade the not-imported precursor protein. Reaction was stopped with PMSF 2.5 mM for 5 min on ice. Samples were centrifuge at 20,000*g* for 10 min at 4 °C and mitochondria were resuspended and washed with 1 ml of HS buffer [500 mM sucrose, 20 mM HEPES/KOH pH 7.4]. Finally, mitochondria were centrifuged at 20,000*g* for 10 min at 4 °C and then lysed under native condition to preserve protein–protein interaction.

Ni-NTA affinity purification

Mitochondria were resuspended in Lysis buffer [50 mM Tris–HCl pH 7.4, 150 mM NaCl, 10% glycerol, 1 mM EDTA, and 1% digitonin] supplemented with 2 mM PMSF and incubated for 20 min at 4 °C. The lysate was clarified by centrifugation at 20,000*g* for 15 min, and the supernatant was incubated with 20 μl of Ni-NTA

Agarose resign (Qiagen) for 2 h at 4 °C with mild rotation. After binding, the resin was washed five times with lysis buffer without digitonin. The column-bound proteins were eluted with Laemmli buffer and analyzed by Western blot.

Proximity ligation assay (PLA)

To monitor the interaction between ectopic APE1 and DNAJc19 in living cells, the *in situ* Proximity Ligation Assay kit (Olink Bioscience) was used. HeLa cells were seated into a glass coverslip in the amount of 8×10^4 per 24-multiwell plate and then fixed with 4% (w/v) paraformaldehyde for 15 min at RT, permeabilized for 5 min with Triton X-100 0.25% in PBS 1X and incubated with 5% normal goat serum in PBS-0.1% (v/v) Tween20 (blocking solution) for 30 min, to block unspecific binding of the antibodies. Cells were then incubated with the mouse monoclonal anti-APE1 (Novus) at a final dilution of 1:400 for 2 h an RT, in a humid chamber. After washing three times with Washing solution [PBS 0.1% (vol/vol) Tween-20] for 5 min, cells were incubated with a rabbit anti-DNAJc19 (Abcam) at a final dilution of 1:400 for 3 h at 37 °C. PLA was performed following manufacturer's instructions. Technical controls, represented by the omission of the anti-DNAJc19 primary antibody, resulted in the complete loss of PLA signal. Images were acquired using an upright laser scanning confocal microscope Zeiss LSM700. For the analysis, an average of 35 randomly selected cells per condition were imaged. PLA-spots present in each single cell were then scored using the BlobFinder software (Olink Bioscience) and in the analysis only extranuclear foci were considered. DAPI staining was used to identify cell nuclei.

Statistical analysis

Statistical analysis was performed using the Microsoft Excel. One-way ANOVA was used for three group comparisons and Student's t-test was used for two group comparisons. p values of less than 0.05 were considered as significant, while values less than 0.01 or lower were considered as highly significant.

DECLARATION OF COMPETING INTEREST

The authors declare that they have no known competing financial interests or personal relationships that could have appeared to influence the work reported in this paper.

Acknowledgements

We would like to thank Dr. Stephen Helliwell and the Novartis Institutes for BioMedical Research for providing the stendomycin and Dr. Tomasz Góral from the Centre of New Technologies of the University of Warsaw for his help in setting up confocal PLA experiments.

Funding

This work was supported by grants to CV from the Associazione Italiana per la Ricerca sul Cancro (MFAG 16780), the National Science Centre, Poland via POLONEZ grant agreement 2016/23/P/NZ1/03899, which has received funding from the European Union's Horizon 2020 research and innovation programme under the Marie Skłodowska-Curie grant agreement No 665778, and by "Regenerative Mechanisms for Health" project MAB/2017/2, carried out within the International Research Agendas programme of the Foundation for Polish Science co-financed by the European Union under the European Regional Development Fund (AC), National Science Centre, Poland 2015/19/B/NZ3/03272 (MW).

Author contributions

Conception and design: CV, AC, MW. Data analysis and interpretation: AB, VB, VT, PE, MW, AC, CV. Manuscript writing: VB, AB, CV. Final approval of manuscript: All authors read and approved the final manuscript. Accountable for all aspects of the work: CV.

Appendix A. Supplementary data

Supplementary data to this article can be found online at https://doi.org/10.1016/j.jmb.2020.11.012.

Received 13 May 2020;
Accepted 9 November 2020;
Available online xxxx

Keywords:
apurinic/apyrimidinic endonuclease 1;
mitochondria;
translocase of the inner membrane;
oxidative stress;
mitochondrial DNA

† These authors contributed equally to this work.
‡ La Jolla Institute for Immunology, La Jolla, CA 92037, USA.

Abbreviations used:
AMA, antimycin A; APE1, apurinic/apyrimidinic endonuclease 1; mtAPE1, mitochondrial APE1; BER, base excision repair; mtDNA, mitochondrial DNA; ETC, electron transport chain; IM, inner membrane; IMS, intermembrane space; MIA, mitochondrial IMS assembly; NLS, nuclear localization sequence; MTS, mitochondrial targeting signal; OM, outer membrane; PAM, presequence translocase-associated motor; PK,

proteinase K; PLA, proximity ligation assay; ROS, reactive oxygen species; SOD, superoxide dismutase; TIM23, translocase of the inner membrane; TOM, translocase of the outer membrane

References

1. Papa, S., Martino, P.L., Capitanio, G., Gaballo, A., De Rasmo, D., Signorile, A., Petruzzella, V., (2012). The oxidative phosphorylation system in mammalian mitochondria. *Adv. Exp. Med. Biol.*, **942**, 1–37.
2. Zhao, R.Z., Jiang, S., Zhang, L., Bin, Y.Z., (2019). Mitochondrial electron transport chain, ROS generation and uncoupling (Review). *Int. J. Mol. Med.*, **44**, 3–15.
3. Blesa, J., Trigo-Damas, I., Quiroga-Varela, A., Jackson-Lewis, V.R., (2015). Oxidative stress and Parkinson's disease. *Front. Neuroanat.*, **9**
4. Zhao, Y., Zhao, B., (2013). Oxidative stress and the pathogenesis of alzheimer's disease. *Oxid. Med. Cell. Longev.*,.
5. Tsutsui, H., Kinugawa, S., Matsushima, S., (2011). Oxidative stress and heart failure. *Am. J. Physiol. - Hear Circ. Physiol.*, **301**, 2181–2190.
6. (2009). Oxidative stress and insulin resistance. J. Japan Diabetes Soc. 49, 845–848.
7. Thanan, R., Oikawa, S., Hiraku, Y., Ohnishi, S., Ma, N., Pinlaor, S., Yongvanit, P., Kawanishi, S., Murata, M., (2014). Oxidative stress and its significant roles in neurodegenerative diseases and cancer. *Int. J. Mol. Sci.*, **16**, 193–217.
8. Roberts, C.K., Sindhu, K.K., (2009). Oxidative stress and metabolic syndrome. *Life Sci.*, **84**, 705–712.
9. Collin, F., (2019). Chemical basis of reactive oxygen species reactivity and involvement in neurodegenerative diseases. *Int. J. Mol. Sci.*, **20**
10. Wang, Y., Branicky, R., Noë, A., Hekimi, S., (2018). Superoxide dismutases: dual roles in controlling ROS damage and regulating ROS signaling. *J. Cell Biol.*, **217**, 1915–1928.
11. Prakash, A., Doublié, S., (2015). Base excision repair in the mitochondria. *J. Cell. Biochem.*, **116**, 1490–1499.
12. Tell, G., Quadrifoglio, F., Tiribelli, C., Kelley, M.R., (2009). The many functions of APE1/Ref-1: not only a DNA repair enzyme. *Antioxid. Redox Signal.*, **11**, 601–619.
13. Jackson, E.B., Theriot, C.A., Chattopadhyay, R., Mitra, S., Izumi, T., (2018). Analysis of nuclear transport signals in the human apurinic/apyrimidinic endonuclease (APE1/Ref1). *Nucleic Acids Res.*, **33**, 3303–3312 http://www.ncbi.nlm.nih.gov/pubmed/15942031.
14. Vascotto, C., Fantini, D., Romanello, M., Cesaratto, L., Deganuto, M., Leonardi, A., Radicella, J.P., Kelley, M.R., et al., (2009). APE1/Ref-1 interacts with NPM1 within nucleoli and plays a role in the rRNA quality control process. *Mol. Cell. Biol.*, **29**
15. Xanthoudakis, S., Miao, G.G., Curran, T., (1994). The redox and DNA-repair activities of Ref-1 are encoded by nonoverlapping domains. *Proc. Natl. Acad. Sci.*, **91**, 23–27.
16. Izumi, T., Mitra, S., (1998). Deletion analysis of human AP-endonuclease: minimum sequence required for the endonuclease activity. *Carcinogenesis*, **19**, 525–527.
17. Wasilewski, M., Chojnacka, K., Chacinska, A., (2017). Protein trafficking at the crossroads to mitochondria. *Biochim. Biophys. Acta – Mol. Cell Res.*, **1864**, 125–137.
18. Barchiesi, A., Wasilewski, M., Chacinska, A., Tell, G., Vascotto, C., (2015). Mitochondrial translocation of APE1 relies on the MIA pathway. *Nucleic Acids Res.*, **43**
19. Stuart, J.A., Hashiguchi, K., Wilson, D.M., Copeland, W.C., Souza-Pinto, N.C., Bohr, V.A., (2004). DNA base excision repair activities and pathway function in mitochondrial and cellular lysates from cells lacking mitochondrial DNA. *Nucleic Acids Res.*, **32**, 2181–2192.
20. Vascotto, C., Bisetto, E., Li, M., Zeef, L.A.H., D'Ambrosio, C., Domenis, R., Comelli, M., Delneri, D., et al., (2011). Knock-in reconstitution studies reveal an unexpected role of Cys-65 in regulating APE1/Ref-1 subcellular trafficking and function Available from *Mol. Biol. Cell*, **22**, 3887–3901 http://www.molbiolcell.org/cgi/doi/10.1091/mbc.E11-05-0391.
21. Li, M., Zhong, Z., Zhu, J., Xiang, D., Dai, N., Cao, X., Qing, Y., Yang, Z., et al., (2010). Identification and characterization of mitochondrial targeting sequence of human apurinic/apyrimidinic endonuclease. *J. Biol. Chem.*, **285**, 14871–14881.
22. Grishko, V.I., Rachek, L.I., Spitz, D.R., Wilson, G.L., LeDoux, S.P., (2005). Contribution of mitochondrial DNA repair to cell resistance from oxidative stress Available from *J. Biol. Chem.*, **280**, 8901–8905 http://www.ncbi.nlm.nih.gov/pubmed/15632148.
23. Barchiesi, A., Wasilewski, M., Chacinska, A., Tell, G., Vascotto, C., (2015). Mitochondrial translocation of APE1 relies on the MIA pathway. *Nucleic Acids Res.*, **43**, 5451–5464.
24. Chacinska, A., Pfannschmidt, S., Wiedemann, N., Kozjak, V., Sanjuán Szklarz, L.K., Schulze-Specking, A., Truscott, K.N., Guiard, B., et al., (2004). Essential role of Mia40 in import and assembly of mitochondrial intermembrane space proteins. *EMBO J.*, **23**, 3735–3746.
25. Zhuang, J., Wang, P., Huang, X., Chen, X., Kang, J., Hwang, P.M., (2013). Mitochondrial disulfide relay mediates translocation of p53 and partitions its subcellular activity. *Proc. Natl. Acad. Sci. USA*, **110**, 17356–17361.
26. Longen, S., Woellhaf, M.W., Petrungaro, C., Riemer, J., Herrmann, J.M., (2014). The disulfide relay of the intermembrane space oxidizes the ribosomal subunit Mrp10 on its transit into the mitochondrial matrix. *Dev. Cell*,.
27. Quinlan, C.L., Gerencser, A.A., Treberg, J.R., Brand, M.D., (2011). The mechanism of superoxide production by the antimycin-inhibited mitochondrial Q-cycle. *J. Biol. Chem.*, **286**, 31361–31372.
28. Vascotto, C., Lirussi, L., Poletto, M., Tiribelli, M., Damiani, D., Fabbro, D., Damante, G., Demple, B., et al., (2014). Functional regulation of the apurinic/apyrimidinic endonuclease 1 by nucleophosmin: Impact on tumor biology. *Oncogene*, **33**
29. Zhang, Y., Wada, J., Hashimoto, I., Eguchi, J., Yasuhara, A., Kanwar, Y.S., Shikata, K., Makino, H., (2006). Therapeutic approach for diabetic nephropathy using gene delivery of translocase of inner mitochondrial membrane 44 by reducing mitochondrial superoxide production. *J. Am. Soc. Nephrol.*,.
30. Filipuzzi, I., Steffen, J., Germain, M., Goepfert, L., Conti, M. A., Potting, C., Cerino, R., Pfeifer, M., et al., (2017). Stendomycin selectively inhibits TIM23-dependent mitochondrial protein import. *Nat. Chem. Biol.*, **13**, 1239–1244.

31. Cadet, J., Davies, K.J.A., (2017). Oxidative DNA damage & repair: an introduction. *Free Radic. Biol. Med.*, **107**, 2–12.
32. Pickering, A.M., Vojtovich, L., Tower, J., Davies, K.J.A., (2013). Oxidative stress adaptation with acute, chronic, and repeated stress. *Free Radic. Biol. Med.*, **55**, 109–118.
33. Lushchak, V.I., (2011). Adaptive response to oxidative stress: bacteria, fungi, plants and animals. *Comp. Biochem. Physiol. - C Toxicol. Pharmacol.*,.
34. Van Houten, B., Santa-Gonzalez, G.A., Camargo, M., (2018). DNA repair after oxidative stress: current challenges. *Curr. Opin. Toxicol.*,.
35. Berdis, A.J., Kelley, M.R. (2012). DNA Repair in Cancer Therapy: Molecular Targets and Clinical Applications.
36. Demple, B., Sung, J.-S., (2005). Molecular and biological roles of Ape1 protein in mammalian base excision repair. *DNA Repair (Amst)*, **4**, 1442–1449.
37. Whitaker, A.M., Freudenthal, B.D., (2018). APE1: A skilled nucleic acid surgeon. *DNA Repair (Amst).*, **71**, 93–100.
38. Santos, J.H., Meyer, J.N., Mandavilli, B.S., Van Houten, B., (2006). Quantitative PCR-based measurement of nuclear and mitochondrial DNA damage and repair in mammalian cells. In: Henderson, D.S. (Ed.), *DNA Repair Protocols: Mammalian Systems*,. Humana Press, Totowa, NJ, pp. 183–199.